JOURNAL OF OPTOELECTRONICS AND ADVANCED MATERIALS, Vol. 11, No. 5, May 2009, p. 547 - 553

Bidirectional S –band continuous wave operation in a depressed-cladding erbium doped fiber amplifier

H. AHMAD*, M. Z. ZULKIFLI, A. A.LATIF, K. THAMBIRATNAM, S. W. HARUN[a]
Photonics Laboratory, Department of Physics, University of Malaya, 50603 Kuala Lumpur, Malaysia.
[a]Department of Electrical Engineering, Faculty of Engineering, University of Malaya 50603 Kuala Lumpur, Malaysia

In this paper we propose and characterize a bi-directional Depressed-Cladding Erbium Doped Fibre Amplifier (DC-EDFA) for Continuous Wave (CW) S-band operation. The system uses a Depressed-Cladding Erbium Doped Fibre (DC-EDF) as the gain medium and 3-port OCs to facilitate bi-directional transmission. The performances of gain and noise figure are first studied for the conventional DC-EDFA setup and are obtained at 20 dB and 4 dB respectively. Subsequently, the bi-directional DC-EDFA is tested and is found to have a similar gain 20 dB but with a slightly higher noise figure of 8.5 dB. The highest gain of 19 dB is obtained for the low input signals of -30 and -20 dBm, while higher input signals of -10 and 0 dB show lower gains due to the on-set of saturation effect in the gain medium. A high noise figure of between 8 and 9 dB is also seen, and increases to 19 dB nearing the cut-off wavelength. The bi-directional EDFA shows no loss in the gain but does show an increase in the noise figure as compared to uni-directional S-band DC-EDFAs.

(Received May 9, 2008; accepted May 25, 2009)

Keywords: Erbium doped fiber amplifier, S-band amplification

1. Introduction

The Erbium Doped Fiber Amplifier (EDFA) provides a very convenient amplification of signals at 1550 nm in existing single-mode optical fibre networks. The EDFA is based on Er^{3+} ions which acts as the active component in the optical amplification process. The EDFA generally features high gain amplification with a low noise figure and has successfully been implemented in the Conventional Band (C-band) region from 1530 nm – 1565 nm as well as the Long-wavelength Band (L-band) from 1565 nm to 1610 nm. The determining factor of these optical network system operating wavelength ranges is the amplification bandwidth of EDFA, which currently spans from 1530 to 1610nm. However, with the steadily increasing usage of bandwidth the need to expand the existing bandwidth is now a serious issue. In this regard, researchers are now focusing on the Short-wavelength Band (S-band) region which ranges from 1480 to 1530 nm, with special attention paid to the development of S-band optical amplifiers. This includes the doping of Er^{3+} ions in telluride that may be able to extend in amplification into the S-band range [1], and also developing an amplification bandwidth covering the S-, C- and L-band regions so as to accommodate the increasing needs of data traffic.

S-band amplification can be achieved either through the use of Thulium doped in Flouride based single-mode fibres or Depressed-Cladding Erbium Doped Fibers (DC-EDFs). Thulium Doped Fibre Amplifiers (TDFAs) employ pumping schemes based either on the conventional upconversion technique using 1050 nm pump laser [2] or using two lasers, one near to 1050 or 1400 nm and the other at 1550nm [3, 4]. However, TDFAs are disadvantageous due to splicing issue with regard to the fluoride based fibre as well as expensive pump lasers. DC-EDFAs however are not susceptible to these problems, as they utilize conventional EDFA components [5, 6] to provide optical amplification in the S-band region. The normal gain of the DC-EDFA is between 15-16 dB with a noise figure of 7-8 dB, and methods such as the double pass S-band EDFA [7, 8] provide significant gain enhancement albeit with a noise figure penalty. The double-pass DC-EDFA is in actuality a uni-directional device, with the signal being reflected back into the gain medium and as such is not truly a bi-directional optical amplifier.

In this paper, we report for the first time a depressed-cladding S-band optical amplifier which uses a single core optical fibre to transmit signals in opposite directions. Although earlier works on bidirectional C-band and L-band EDFA optical amplifiers have been reported [9, 10], there is no detailed reporting of S-band bidirectional EDFA. S-band bidirectional optical amplifiers would find applications in networks that have exhausted their optical fiber pairs. Bidirectional traffic allows the use of a single fibre core to carry traffic in both directions and thus doubles the carrying capacity of the network or even provides a spare core for protection propose [11].

2. Experiment setup

In designing the bi-directional S-band DC-EDFA, a methodological characterization of the each stage of the development of the bi-directional amplifier is done. Because the bi-directional amplifier is developed from the conventional uni-directional S-band DC-EDFA, a proper

understanding of the behavior of the conventional amplifier will allow for the smooth development of the bi-directional DC-EDFA. Fig. 1 (a) shows the setup of the conventional S-band EDFA. The setup uses a 15 m DC-EDF with a fundamental cut-off wavelength of 1525 nm (although the cut-off wavelength can be adjusted by changing on the spooling radius) and an Er^{3+} ion concentration of 440 ppm. A 980 nm Laser Diode (LD) with an output power of 100 mW is used to optically pump the Er^{3+} ions in the DC-EDF, while a Wavelength Selective Coupler (WSC) is used to combine the pump and signal wavelengths. The spooling diameter of the DC-EDF is set to 8 cm, as this is determined to be the optimum diameter of the DC-EDF as to maintain a cut-off wavelength of 1525 nm. This spooling radius provides the required amplification bandwidth in the S-band region (1480 – 1520 nm) [12].

Figs. 1 (b) and 1 (c) show the effect of the 3-port Optical Circulator (OC) in the conventional S-band DC-EDFA at different positions of the cavity. Due to its bi-directional the optical circulator is preferred in replacing the optical isolator in the S-band DC-EDFA setup, by allowing signals in one direction to travel straight through and redirecting signals moving in the opposite direction to another leg. In Fig. 1 (b), Port 1 of the OC is connected to the end of the 15 m DC-EDF while Port 2 is connected to the Optical Spectrum Analyzer (OSA). The optical power leak at Port 1 is measured to be 0.5 dB. In this setup, the OC acts as an isolator by allowing only forward propagating signals (which propagate in the same direction as the pump wavelength) to reach the OSA, while backward propagating signals (that propagate in the opposite direction of the pump wavelength) are redirected away by the OC. In Fig. 1 (c), another OC is placed before the WSC, with Port 1 connected to the TLS and Port 2 connected to the WSC to simulate the backward propagating configuration. Again, both OCs prevent backward propagating signals from travelling within the DC-EDFA, and the characterization of the S-band DC-EDFA is necessary as this design will be used as the basis for the bi-directional S-band DC-EDFA.

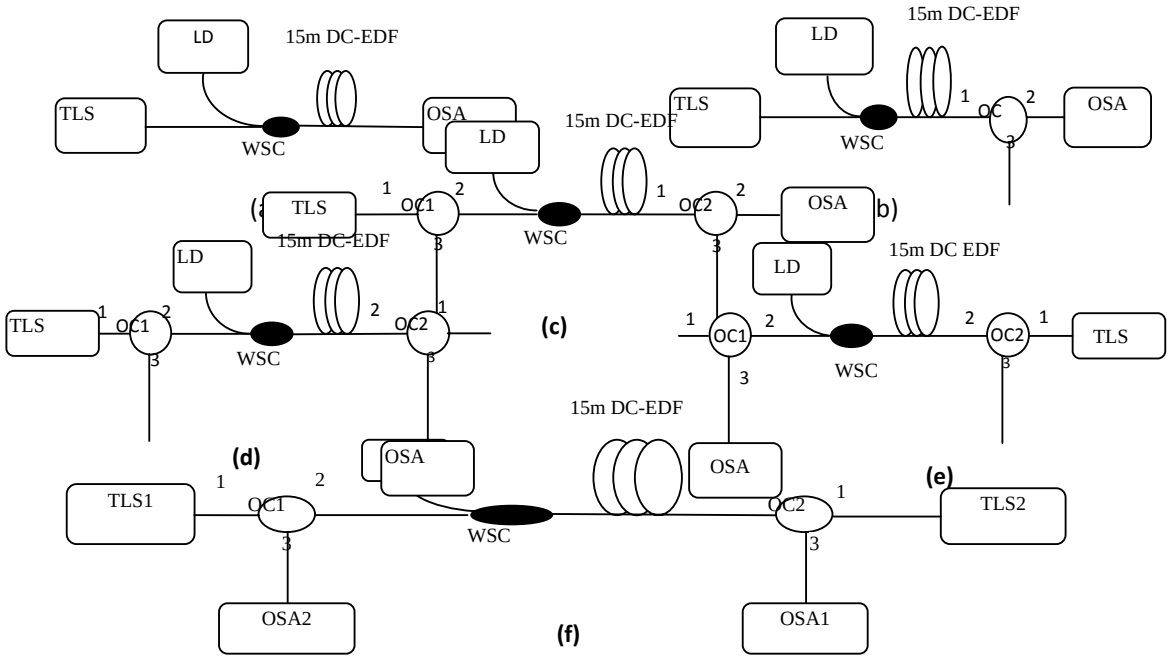

Fig. 1. (a) Conventional S-band DC-EDFA with forward pumping configuration, (b) conventional S-band DC-EDFA with forward pumping configuration with an optical circulator at the output end, (c) conventional S-band DC-EDFA with forward pumping configuration with optical circulators at both the input and output ends, (d) Bi-Directional S-band DC-EDFA with forward signal only (same direction with the pump), (e) Bi-Directional S-band DC-EDFA with backward signal only (opposite direction of pump) and (f) Bi-Directional S-band DC-EDFA with both signals travelling in opposite directions in the optical amplifier in the same single mode optical fibre

Before the behavior of the bi-directional S-band DC-EDFA can be examined, it is necessary to understand how the S-band DC-EDFA performs in forward or backward signal propagation. Fig. 1 (d) shows the setup for the bi-directional S-band DC-EDFA with forward propagating signal only. The S-band DC-EDFA is setup as in Fig. 1 (c), with port 1 of OC1 connected to the TLS and Port 2 connected to the WSC. Port 2 of OC 2 is connected to the 15 m DC-EDF, while Port 3 is connected to the OSA. In this manner, a forward propagating signal is simulated from a TLS will enter Port 1 and then Port 2 of OC1, which then passes the gain medium and reaches Port 2 of OC2. The signal then travels from Port 2 to Port 3 and to the OSA. Fig. 1 (e) on the other hand shows the bi-

directional S-band DC-EDFA with a backward propagating signal only, whereby the TLS is now connected to Port 1 of OC2 and the OSA is connected to Port 3 of OC1. Port 2 of OC2 is connected to the gain medium, while Port 2 of OC1 is connected to the WSC. The simulated backward propagating signal travels from the TLS to enter Port 1 through Port 2 of OC2, where it then enters the gain medium and subsequently passes Port 2 through Port 3 of OC1 to reach the OSA. The final configuration of Fig. 1 (f), the bi-directional S-band DC-EDFA is setup for both the forward and backward signals to propagate simultaneously by combining the setups of Figs. 1 (d) and 1 (e). All fibres joints are made using a commercially available fusion splicer with the splicing loss controlled to under 0.03dBm. The S-band TLS' have a wavelength range 1460 nm - 1530 nm while the OSAs used have a 0.01 nm resolution. A specially designed automation software [13] is also used to increase accuracy and reduce experiment time.

3. Results and discussion

Before characterization on the bi-directional amplifier can begin, the conventional uni-directional DC-EDFA is first characterized. Fig. 2 shows the amplified spontaneous emission (ASE) of the conventional S-band EDFA. At a wavelength of 1510 nm the peak ASE power is obtained at – 30 dBm. Given that the cut-off wavelength is around 1525 nm, wavelengths loner than 1514 nm are suppressed, allowing for the S-band signals to receive more ASE for amplification. The attainable S-band gain is limited however due to the high ASE that still exists in the 1530 nm region, although this ASE depends on the spooling diameter of the DC-EDFA and the experimental setup (which can include filters to completely remove the unwanted ASE).

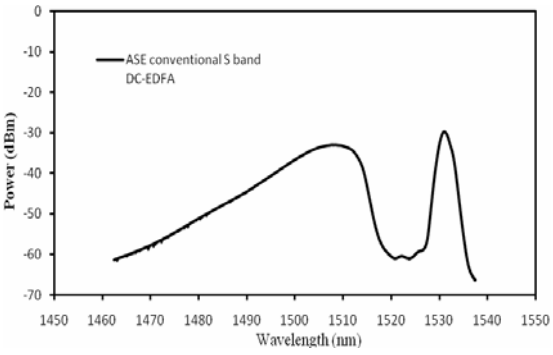

Fig. 2. ASE spectrum of conventional S- band DC-EDFA (for the setup of Fig. 1 (a)).

Fig. 3 shows the gain and noise figure of the conventional S-band EDFA against input powers from -40 dBm to 5 dBm at 1500 nm. The highest gain obtained is 18.37 dB at the region of the lowest input signal power (– 40 dBm). The gain at this region is flat and remains high until an input power of -20 dBm, after which it begins to drop to only 5.25 dB at an input signal of 5 dBm. The drop in the gain is due to the saturation of the gain medium caused by the high power input signal. The noise figure shows a similar trend, remaining flat at approximately 8 dB through an input signal range of – 40 to 0 dBm and increases to 8.86 dB at an input power of 5 dBm. The high noise figure is also caused by the saturation of the gain medium brought about by the high power of the input signal. These results show that the conventional S-band EDFA functions well as an amplifier at distances far from the source signal (where the power is low, between – 20 dBm and -40 dBm), but is not particularly effective near the source signal (where the high input signal powers of above -20 dBm).

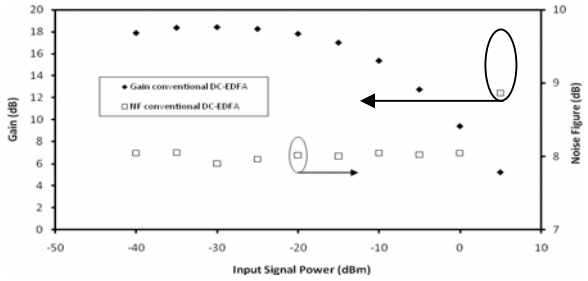

Fig. 3. Gain and Noise Figure as a Function of the Input Power for the S-band DC-EDFA Setup with a Center Wavelength of 1500nm (for the setup of Fig. 1 (a)).

Fig. 4 shows the gain and noise figure of the conventional S-band EDFA against different wavelengths at a set of input power of -30 dBm. The wavelength ranges from 1480 nm to 1532 nm in 4 nm increments. As observed in the figure, the gain of the conventional S-band EDFA is low at the shorter wavelengths. As the input signal wavelength moves towards the longer wavelengths, the gain also increases until a maximum gain of 23.71 dB is achieved at 1508 nm, which corresponds to the peak ASE as observed in Fig. 2. After 1508 nm, the gain drops drastically to only 3.17 dB at 1512 nm, while no gain is observed for wavelengths above 1520 nm due to the cut-off wavelength. As the wavelength approaches the cut-off wavelength, the optical wave is no longer guided by the core but instead travels in the cladding, resulting in a considerable loss in the signal strength [14] and thus the lack of gain. The noise figure of the EDFA remains relatively constant between 8.3 dB and 7.5 dB throughout the wavelength range. After 1520 nm, the noise figure cannot be computed due to the absence of gain in the medium.

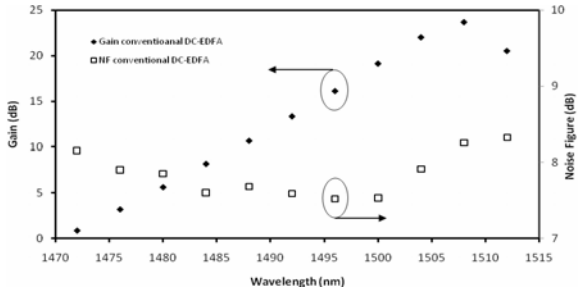

Fig. 4. Gain and Noise Figure as a Function of Wavelength for the Basic DC-EDFA Setup with an Input Power of -30dBm (for the setup of Fig. 1 (a)).

Fig. 5 on the other hand shows the gain and noise figure of the same S-band EDFA against different wavelengths at a higher input power of 0 dB. While it can be seen from Figure 5 that the gain and noise figure spectrum is similar to that of conventional S-band for low signals, the overall gain for high input signals is only 9.90 dB as opposed to the 23.71 dB gain that is obtained by the low signal. This drop in the gain is due to the saturation induced power effect on the DC-EDF, which also contributes to the slightly higher noise figure as seen in Fig. 5.

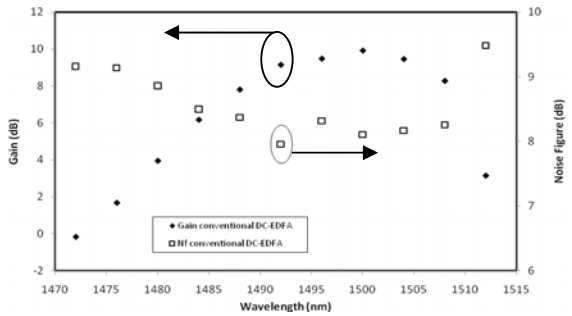

Fig. 5. Gain and Noise Figure as a Function of Wavelength for the Basic DC-EDFA Setup with an Input Power of 0 dBm (for the setup of Fig. 1 (a)).

Fig. 6 shows the performance of the gain and noise figure against different input signal powers for the S-band EDFA setup with no OC, one OC and two OCs (for the setups of Figs. 1 (a), 1 (b) and 1 (c)). The effect of the OC on the amplifier must be studied, as this configuration will form the basis of the bi-directional S-band DC-EDFA. The center wavelength of the test signal is fixed at 1500 nm. As can be seen in the figure, all three configurations show a similar pattern with a relatively flat gain of 18 dB for an input signal range of -40 dBm to -15 dBm. At this region only a 0.83 difference in the gain is seen between all three configurations. After – 15 dBm however the EDFA becomes saturated, causing the gain to drop. It can be seen that while the placement of the OCs has no effect on the gain of the EDFA, it does have an effect on the amplifier's noise figure. The conventional S-band EDFA has the lowest noise figure pattern of all three configurations of 7 dB, while the S-band EDFA with two OCs has the highest noise figure of 9 dB. This difference can be attributed to the wavelength sensitive insertion loss of the OC (which has an operational wavelength of 1550 nm) which reduces the signal power and increases the noise figure.

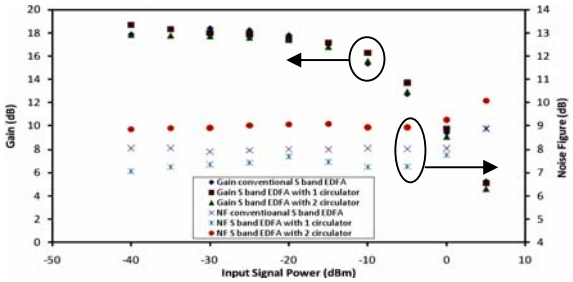

Fig. 6. Gain and Noise Figure as a Function of the input power (For the setups of Figures 1 (a), (b) and (c)).

Fig. 7 on the other hand shows the gain and noise figure performance of the conventional S-band EDFA and S-band EDFAs with the OCs at a low input power against different wavelengths. As with the case of Figure 6, the gain spectrum and noise figure spectrum of all three configurations is similar. The gain of the conventional S-band EDFA is only slightly higher, by about 0.99 dB as compared to the other two setups. However, the noise figure for conventional setup and setup with one OC is similar while the noise figure for the setup with two OCs is higher by about 1 dB due to the wavelength dependence of both of OCs. Fig. 8 show that the three configurations exhibit the same behavior when exposed to a high input power against different wavelengths.

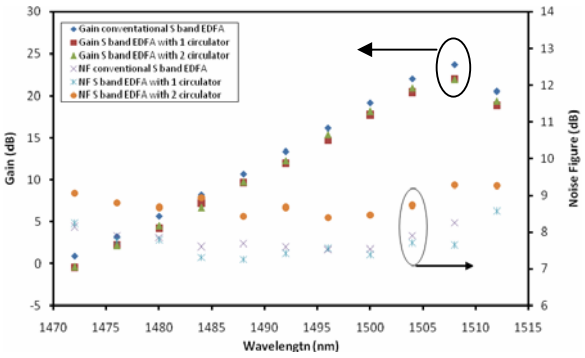

Fig. 7. Gain and noise figure against wavelength for a low input signal of – 30 dBm (For the setups of Fig. 1 (a), (b) and (c)).

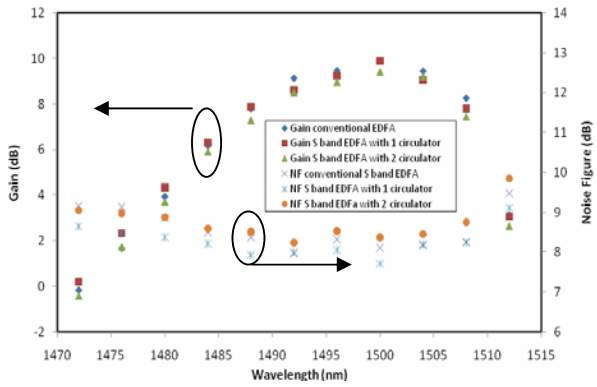

Fig. 8. Gain and noise figure against wavelength for a low input signal of -30 dBm (For the setups of Fig. 1 (a), (b) and (c)).

Fig. 9 shows the ASE spectrum of the S-band EDFA in both the forward and backward configurations. The ASE spectrum of both configurations is observed to be similar, with peaks at 1510 nm and 1530 nm and a dip at 1520 nm. The forward configuration ASE spectrum is higher by approximately 10 dB as compared to the backward configuration ASE spectrum because of the forward pumping configuration of the DC-EDF. In this configuration, the forward end of the DC-EDF has a very high population inversion due to its proximity to the optical pump source as compared to the backward end of the DC-EDF. As such, the ASE generated from the forward end of the EDF is higher than the ASE generated from the back end of the DC-EDF.

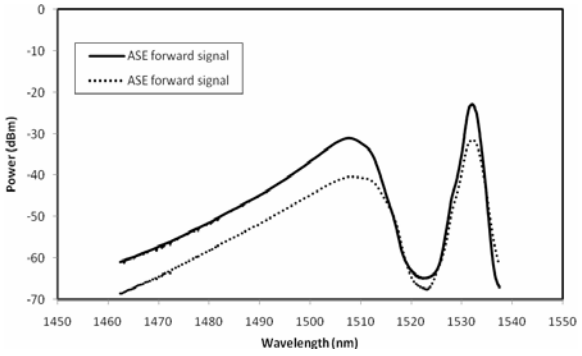

Fig. 9. ASE spectrum of the S-band EDFA in both the forward and backward configurations. (For the setups of Fig. 1 (d) and (e)).

Fig. 10 shows the gain and noise figure for forward and backward propagating signals along the DC-EDF against a fixed wavelength. Similar to the ASE spectrum, the gain of the backward propagating signal is lower than that of the forward propagating signal, with a difference at a magnitude of 10 dB. This difference in the gain corresponds to the difference of power of the ASE signal, which is expected as the limit of the ASE will in turn determine the limit of gain available. The noise figure of the backward signal is lower than that of the forward signal, due to lower ASE power available.

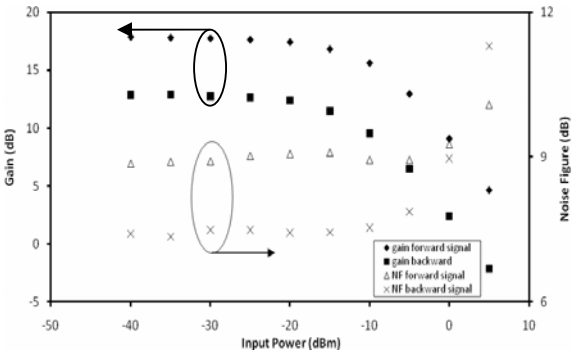

Fig. 10. Gain and noise figure value against input power at center wavelength 1500 nm (For the setups of Figures 1 (d) and (e))

Figs. 11 and 12 show the gain and noise figure of the forward and backward propagating signals against different wavelength for the case of low and a high input signal powers. In Figure 11, the power of both the forward and backward input signal is set to a low signal power which is– 30 dBm. As can be seen both the forward and backward signals have the same gain spectrum which peaks at 1507 nm. However, the gain of the forward signal is higher than the gain of the backward signal, again due to the difference in the ASE power available. The noise figure of the forward and backward signals on the other hand is relatively flat, with no significant difference in the noise figure. This is not expected as the noise figure is predicted to be high due to the difference in the gain. The same situation is also seen in Figure 12 for the high input signal of 0 dBm. The gain peaks at approximately 1500 nm, with the gain of the forward propagating signal approximately 10 dB higher than that of the backward propagating signal.

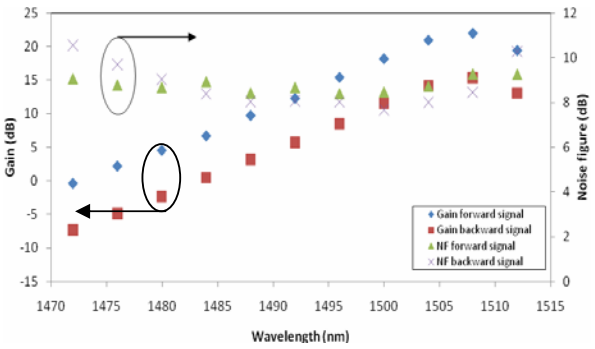

Fig. 11. Gain and noise figure value against different input wavelengths at fixed -30 dBm input signal (For the setups of Figs. 1 (d) and (e)).

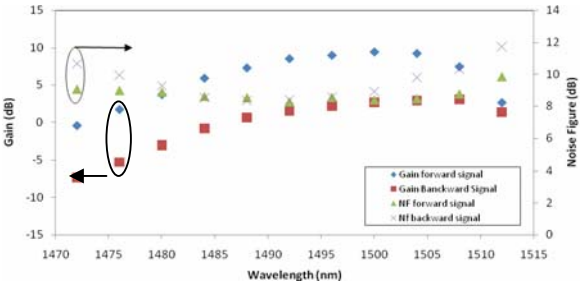

Fig. 12. Gain and noise figure value against different input wavelengths at fixed 0 dBm input signal (For the setups of Figs. 1 (d) and (e)).

In the characterization of the bi-directional S-band EDFA, the setups as in Figures 1 (d), 1 (e) and 1 (f) are used. For the purpose of this experiment, the TLS generating the forward signal is designated as TLS1 and is connected to Port 1 of OC1, while the TLS generating the backward signal is designated as TLS2 and is connected to Port 1 of OC2. Two OSAs are used to analyze the bi-directional S-band EDFA, namely OSA1 which connected to Port 3 of OC2, and OSA2 which is connected to Port 3 of OC1. OSA1 s used to analyze the forward propagating signal from TLS1, while OSA2 analyzes the backward signal from TLS2.

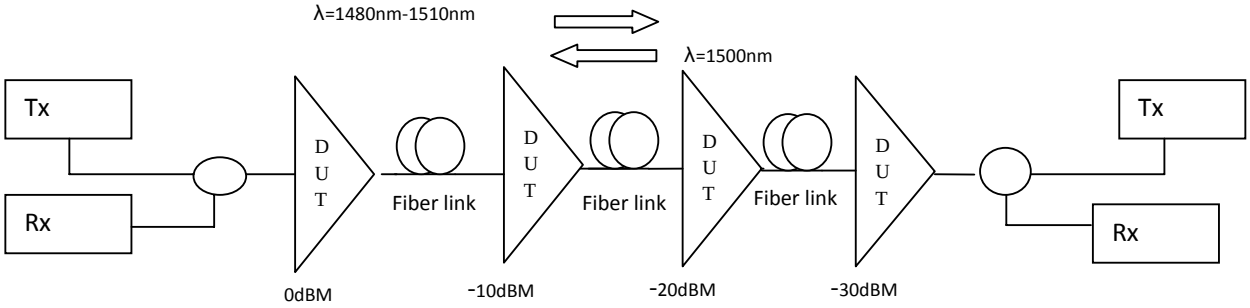

Fig. 14. Simulated location of bi-directional S-band EDFA based on changing input powers

For the characterization of the bi-directional S-band DC-EDFA, TLS2 set at a constant -30dBm with center wavelength 1500 nm while the input wavelength and power of TLS1 is changed from -30dB to 0dB is to simulate the bi-directional S-band EDFA as an in-line amplifier for long-haul transmissions, a pre-amplifier a booster amplifier and also as an in-line amplifier for short-haul networks. Fig. 14 illustrates this point.

Fig. 15 shows the gain of the bi-directional S-band EDFA against different wavelengths for input powers of -30 dBm, -20 dBm, -10 dBm and 0 dBm. The gain of the EDFA is observed to be similar to that of the S-band in a forward or backward configuration, with the peak gain seen at 1505 nm. Off the four input signals, the input signal with the lowest power experiences the highest gain, which in this case is the -30 dBm input signal which has a gain of almost 20 dB. The gain of the -20 dBm signal is also significant and is approximately 19 dB. However, as the input signal power increases, the gain experienced by the signal reduces, due to the saturation of the DC-EDFA. The input signal of -10 dBm shows a lower gain of 15 dB as compared to the -30 dBm and -20 dBm signals, while the lowest gain is observed for the 0 dBm signal, which is only 8 dBm. Due to the fundamental cut-off of the S-band DC-EDFA, no gain exist for either signal after 1510 nm, as the signals are now travelling in the high loss cladding regions.

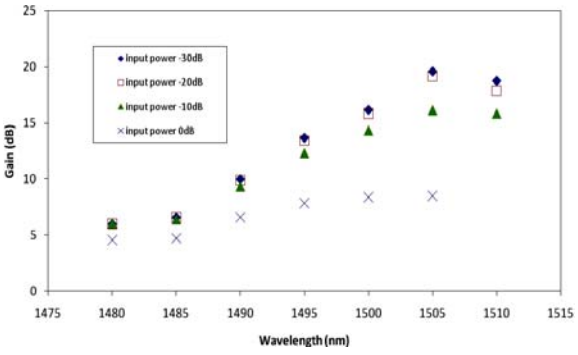

Fig. 15. Gain of bi-directional S-band EDFA against wavelength for different input powers (for the setup as in Fig. 1 (f)).

The noise figure spectrum of the S-band EDFA against different signal wavelengths is shown in Figure 16. It can be seen that the noise figure for all four input signals is relatively flat between 8 and 9 dB at a wavelength range of 1480 nm to 1505 nm. The highest noise figure is seen by the 0 dBm signal, which is expected as this signal

experiences the lowest gain. The noise figure of the other three input signals fluctuates but remains close to one another. As the wavelength region approaches the cut-off wavelength, the noise figure rises due to the loss of gain, and after 1510 nm the noise figure cannot be computed.

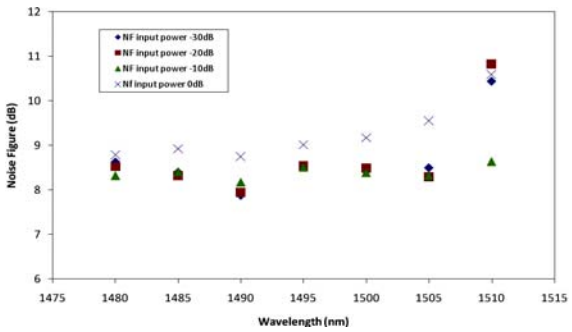

Fig. 16. Noise figure of bi-directional S-band EDFA against wavelength for different input powers (for the setup as in Fig. 1 (f)).

Therefore, the bi-directional S-band EDFA is shown to be capable of amplifying bi-directional CW signals with no loss in the gain as compared to uni-directional S-band EDFAs. However, a noise figure penalty is observed for both the forward and backward signals due to the addition of the two OCs. This amplifier has many potential applications in new S-band networks as well as in combination with C- and L-band amplifiers for use in ultra wideband systems.

4. Conclusion

A bi-directional EDFA for CW S-band amplification is proposed and demonstrated. The system consists of a DC-EDF to obtain amplification in S-band region and 3 port OCs to facilitate bi-directional transmission. The performances of gain and noise figure are first studied for different conventional setup configurations, and the gain and noise figure is obtained at 20 dB and 4 dB respectively. The bi-directional EDFA on the other hand has a similar gain 20 dBm but a higher noise figure of 8.5 dB. The highest gain of 19 dB is obtained for low input signals of -30 and -20 dBm, while higher input signals of -10 and 0 dB show relatively lower gains due to the saturation of the gain medium. A high noise figure of between 8 and 9 dB is seen however for all signal powers, with the highest noise figure of 11 dB seen near to the cut-off wavelength. The bi-directional EDFA shows no loss in the gain but does show an increase in the noise figure as compared to uni-directional EDFAs.

References

[1] T. Sakamoto, A. Mari, H. Masuda, H. Ono, NTT Technology Review **2**(12), 38
[2] F. Roy, OFC 2002, Anaheim, CA, 2003, postdeadline paper PD2-1
[3] T. Kasamatsu, Y. Yano, T. Ono, IEEE Photon. Technol. Lett., **13**, 433 (2001).
[4] "Gain shifted dual-wavelength pumped Thulium doped fibre amplifier from WDM signals in the 1.48-1.51 μm wavelength region", IEEE Photon. Technol. Letts, **13**, 31 (2001).
[5] M. Abore, Y. Zhon, H. Thiele, J. Bromage, L. Nelson, OFC 2003, Anheim Ca
[6] H. Ono. A. Yamada, N. Shimiju, Electronics Letters, **38**, 1084 (2002).
[7] H. Ahmad, S. W. Harun, Journal of Nonlinear Optical Physics and Materials, **15**, 303 (2006).
[8] S. W. Harun, H. Ahmad, Optics and Laser Technology, **39**, 935 (2007).
[9] C. W. Barnard, J. Chrostowsla, M. Karchrad, IEEE Photon Technol. Letts, **4**, 911 (1992).
[10] M. A. Mahdi, F. R. M. Adikan, P. Poopalan, S. Selvadurai, H. Ahmad, OFC 2000, **1**, 8 (2000).
[11] D. Zhou, S. Subramaniam, Survivability in optical networks, IEEE Networks, **14**(6), 16 (2000).
[12] H. Ahmad, N. K. Saat, S. W. Harun, Laser Phys. Lett. **2**, 412 (2005).
[13] M. Z. Zulkifli, S. W. Harun, K. Thambiratnam H. Ahmad, Accepted for publication in IEEE Instrumentation and Measurement Journal, 2007
[14] L.G. Cohen, D. Marcuse, W. L. Mammel, Microwave Theory and Techniques, IEEE Transactions on, 1982.

*Corresponding author: harith@um.edu.my